Received: 23 August 2024 | Revised: 19 December 2024 | Accepted: 15 January 2025 | Published online: 5 February 2025

RESEARCH ARTICLE

Medinformatics
2025, Vol. 2(3) 205–218
DOI: 10.47852/bonviewMEDIN52024158

BON VIEW PUBLISHING

Combinatorial Design of Imidazole/Triazole Linked Aryl-Substituted Derivatives as CYP17 Inhibitors Exploring Hansch and Molecular Docking Approach

Balaji Wamanrao Matore[1], Anjali Murmu[1], Jagadish Singh[1] and Partha Pratim Roy[1,*]

[1]*Department of Pharmacy, Guru Ghasidas Vishwavidyalaya, India*

Abstract: Prostate cancer is one of the most common age-related cancers, characterized by uncontrolled cell growth that develops in the walnut-sized prostate gland in men, which potentially forms tumors and metastases to other parts of the body if it is untreated. It is widely recognized that 80% of prostate cancers are androgen-dependent. Thus, inhibition of CYP17 hydroxylase and lyase will stop the androgen synthesis and testosterone overproduction and ultimately help in treating prostate cancer. Heterocyclic scaffolds (especially imidazole and triazole) have great affinity and potency against the CYP17 hydroxylase and lyase. In this study, we developed a statistically robust and reliable predictive model using Hansch and topological parameters with a series of phenyl alkyl imidazole-based 17α-hydroxylase/17-20-lyase inhibitors. The promising scaffolds were optimized based on the mechanistic interpretations of substitutions, fragments, and branching, and a total of 3645 novel compounds were designed and screened over topological models to identify drug-like potential inhibitors. Molecular docking analysis depicted binding patterns, interaction energies, and a possible mechanism of inhibition of potential molecules. Finally, six potential hydroxylase and nine lyase inhibitors were reported based on the docking score and binding free energy. The novel 369 and 318 are the most promising designed candidates for prostate cancer treatment, while the compound 625 is a potential selective lyase inhibitor with 375-fold activity over the hydroxylase. The ADMET study states the compounds are drug-like and non-toxic. The findings of this study will help experimental researchers with a prior basis for the potential of novel, promising CYP-17 inhibitors of this class.

Keywords: CYP17 hydroxylase and lyase, imidazole, docking, QSAR, Hansch modeling

1. Introduction

Prostate cancer is an age-related disease and the second leading cause of cancer in the western countries [1, 2]. It is now widely recognized that majority of the prostate cancers are androgen-dependent [3, 4]. The cytochrome b5-modulated key enzyme 17α-hydroxylase/17-20-lyase (CYP17) for androgen synthesis catalyzes the last two sequential reactions in the production of testosterone, such as (i) 17α-hydroxylation and (ii) subsequent C17–C20 bond cleavage of pregnenolone and progesterone to form Dihydroandrostenedione and androstenedione, the precursors of testosterone [5–8]. Thus, targeting the enzyme of interest (CYP17) for the treatment of androgen-dependent prostate cancer could be a promising alternative [9–11]. Ketoconazole and Abiraterone are the only approved CYP 17 inhibitors which have been used in advanced prostate cancer, while Orteronel, Galeterone (TOK-001), and VT-1129 are the investigational drugs [12–15]. Efforts have been made during the years to develop non-steroidal CYP17 inhibitors due to side effects of steroidal inhibitors related to their backbone structure [16–18]. The recent studies described that the incorporation of nitrogen-containing heterocyclic scaffolds has great affinity and potency against the CYP17 hydroxylase and lyase [19–22]. Nowadays, heterocyclic scaffolds are widely included in novel anticancer agents [23–26]. The azole category compounds have acquired great attention (especially imidazole and triazole) due to their potentiality [27–29]. The optimization of these scaffolds is necessary to find out more potential drug-like candidates.

Over the years, various strategies are adopted in designing CYP17 inhibitors, and some of the key and necessary parameters should be considered while designing novel compounds [21, 30, 31]. Basic nitrogen-containing heterocyclic scaffolds, iron coordination, and the distance between the iron-nitrogen (Fe-N) are playing pivotal roles in producing inhibitory action [32–35]. For example, Abiraterone and Galeterone are the co-crystal ligands bound with 3RUK and 3SWZ [36] proteins and have found Fe-N distance 2.04 and 2.22 Å, respectively. It is better to perform the molecular docking study to find or analyze the Fe-N coordination, and it plays a crucial role in designing novel CYP17 inhibitors [31, 36–38].

Followed by the design of scaffolds, it is essential to substitute influential substituents to improve the potential and optimize the scaffolds or lead molecules [39, 40]. Hansch parameters have already strong ability to find out the contribution of major as well

***Corresponding author:** Partha Pratim Roy, Department of Pharmacy, Guru Ghasidas Vishwavidyalaya, India. Emails: parthapratim.roy@ggu.ac.in; partha.r.in@gmail.com

as very small substitutions for more than six decades [41–43]. Along with the Hansch parameters, topological and indicator parameters also play an important role in understanding the substitution effect [4, 44].

In continuation of our previous publication for the present study, a series of phenyl alkyl imidazole-based derivatives having 17α-hydroxylase/17-20-lyase inhibitory activities were collected from literature to explore the physicochemical and structural features of the compounds in their selectivity as well as inhibitory activities [45–51].

The primary objective of the study is to develop a statistically robust and reliable predictive model using Hansch and topological parameters and to explore the effect of substitutions on CYP17 inhibitory activity. The second objective is to optimize and design scaffolds as well as a combinatorial library by incorporating influential substitutions and finally to predict the inhibitory activity, molecular mechanism, and binding affinity of designed promising novel compounds to identify potential CYP17 hydroxylase and lyase inhibitors.

2. Material and Methods

2.1. Dataset and descriptors

Inhibitory activities of a series of phenyl alky imidazole/triazole substituted derivatives (Table S1) against the human 17α-hydroxylase/17-20-lyase (CYP17) enzyme reported in the literature have been used as the model dataset for the present QSAR analysis [16, 52–54]. The inhibitory potencies of the compounds [IC_{50} (μM)] have been converted to the logarithmic scale [pIC_{50} (μM)]. The dataset of 51 compounds used for modeling with their pIC_{50} values was reported in Table S1. The structures were drawn in ChemBioDraw and subjected to an energy minimization using a smart minimizer and a CHARMn force field to generate the lowest energy conformations. All the descriptors were calculated using Discovery Studio Client 4.1 (DSC 4.1) software. Definitions of all descriptors can be found at the Discovery Studio Client tutorial available at the website https://www.3ds.com/ [55]. For classical QSAR analysis using a linear free energy related model of Hansch [56]. We have taken the lipophilicity constant (π), electronic constant (Hammett σ), and steric (molar refractivity (MR) and STERIMOL L, B1, and B5) parameters of the aryl ring substituents along with appropriate indicator parameters. Different physicochemical and indicator variables used in the study have been defined in Table S2. The values of the physiochemical substituent constants (Table S3) were taken from Achary [57]. In addition, QSAR models were developed from topological descriptors.

2.2. Model development

The total number of compounds for the dataset for both activities containing 51 compounds (42 and 48 CYP17 hydroxylase and lyase inhibitors, respectively) was first divided into two subsets by the k-means clustering technique based on a standardized topological, structural, and physicochemical descriptor matrix [58, 59]. The numbers of compounds for the training sets (topological) were 31 and 36 for CYP17 hydroxylase and lyase, respectively, and the test sets were composed of 12 and 11 compounds for CYP17 hydroxylase and lyase, respectively. In the case of the Hansch method, training and test sets for hydroxylase are 24 and 9, respectively, and for lyase 29 and 10, respectively. The rest of the compounds in the dataset were lacking common scaffold and hence omitted from the analysis. GFA was used as a chemometric tool for model development [60].

2.3. Statistical qualities

The statistical qualities of the equations were judged by the parameters such as *determination coefficient* (R^2) and *variance ratio* (F) at specified *degrees of freedom* (df) [61]. The generated QSAR equations were validated by leave-one-out *cross-validation* R^2 (Q^2) and *predicted residual sum of squares* [62, 63]. The prediction qualities of the models were judged by statistical parameters like Q^2F_1, Q^2F_2, CCC_{ext}, and r^2m_{avg} [64, 65].

2.4. Designing of novel potential CYP17 hydroxylase and lyase inhibitors

The combinatorial library of novel CYP17 hydroxylase and lyase inhibitors was designed by using the mechanistic interpretation of the Hansch model (Equations (1) and (2)) and the topological model (Equations (3) and (4)). The scaffolds were optimized, and different substituents like OH, Cl, F, Br, -CH_2-OH, methyl, ethyl, propyl, and isopropyl were substituted on the *para* and *meta* positions of the phenyl ring. A total of 3645 novel CYP17 hydroxylase and lyase inhibitors were designed using SmiLib software [66].

2.5. Activity prediction and finding of potential hits

All the designed compounds were minimized in DSC 4.1 and subjected to descriptor calculations. Further, these compounds were screened over the topological model of hydroxylase and lyase to predict the theoretical IC_{50} value. Different cut-offs like HAT value, IC_{50} less than most potent compound of dataset, and standards to identify some potential hits.

2.6. Molecular docking

The molecular docking of potential hits was performed to analyze the binding pattern, mechanism of action, and the different types of favorable interactions [67, 68]. The 3ruk protein was downloaded from the protein data bank and prepared by adding hydrogen, deleting water, adjusting pH 7.4, adding missing residues, and cleaning protein structure [47]. The protein structure was minimized using the smart minimizer and the CHARMm force field. The binding site was selected based on the co-crystal position, and the X, Y, and Z coordinates are 27.887, −5.724, and 34.447, respectively. The docking of co-crystal ligand was performed using the LibDock algorithm to validate the protocol [31]. Following validation, all potential hits were docked over the 3ruk protein, and the different parameters were analyzed. The whole process was performed in DSC 4.1, and the detailed protocol was discussed elsewhere [31].

2.7. Binding free energy calculation

The binding free energy calculations for best-docked poses were performed using the DSC 4.1. During the process, *in situ* energy was kept true, and the remaining default parameters were used. The different energy parameters, like binding free energy, ligand conformational energy, and complex energy, were generated [57].

3. Results and Discussion

3.1. Modeling with physicochemical descriptors

Equations (1) and (2) are the best equations obtained from GFA (5000 iterations) for hydroxylase and lyase inhibitory activity,

Table 1. Statistical qualities of developed models

Model	Training/ Test	R^2	R^2_{adj}	Q^2_{loo}	Q^2F_1	Q^2F_2	r^2m_{ave}	CCC_{ext}	MAE_{ext}
Hansch Model									
Model-1	24/09	0.903	0.889	0.830	0.879	0.879	0.841	0.935	0.279
Model-2	29/10	0.945	0.934	0.903	0.858	0.832	0.694	0.903	0.219
Topological Model									
Model-3	31/11	0.929	0.921	0.911	0.842	0.908	0.852	0.904	0.308
Model-4	36/12	0.896	0.600	0.788	0.867	0.858	0.854	0.940	0.241

respectively. Both linear and spline terms were used to develop the QSAR models. The scatter plot for the hydroxylase models 1 and 3 are shown in Figure S1 and for lyase models 2 and 4 are shown in Figure S2. The statistical qualities of Equations (1) and (2) are listed in Table 1 along with other developed models and found to be significant both internally and externally.

3.1.1. Hydroxylase Hansch model

$$\begin{aligned} pIC_{50-OHase} = & -0.262\ (\pm 0.138) \\ & +\ 0.424\ (\pm 0.032)\ <7-\ Integer> \\ & -0.944(\pm 0.196)\ MR_p \\ & -\ 0.426\ (\pm 0.236)\ MR_m \end{aligned} \quad (1)$$

The term *Integer* represents the number of alkyl groups connecting the phenyl and azole ring. The term <7-*Integer*> with a negative regression coefficient indicates that for optimal hydroxylase inhibitory activity, the numerical value of an integer should be equal to or greater than 7 (e.g., **25**, **27**, **31**) than compounds with one (like compounds **2, 9, 10, 11**) or two (like compounds **17, 19**) alkyl groups in between phenyl rings. An increase in the number of alkyl groups indicates an increase in molecular hydrophobicity. It was stated in the source papers that LogP plays an important role in the inhibitory activity, which is supported by our study. The steric parameter MR of substituents has a positive impact both in the *para* and *meta* positions of the phenyl ring. Compounds with lower numerical MR_p values like **2, 11,** and **17** showed significantly lower inhibitory activities than compounds (**28, 29**) with higher MR_p values. But it was observed that compounds (like **3, 4, 5, 6, 7, 14**) showed poor inhibitory activities instead of higher values of MRp due to a smaller number of integer values ($n = 1$). The structural alerts from model 1 for compounds 25, 10, 17, 31, 2, and 28 are highlighted in Figure 1(A). For the term MR_m, only compounds like **10, 11, 13,** and **14** have OCF_3, Cl, F, and Br substitutions at the meta position, respectively, and posses a higher value of MR. It showed significantly lower activity because only one alkyl group separated the phenyl and azole ring, and the integer value is 1 for all the compounds.

3.1.2. Lyase Hansch model

$$\begin{aligned} pIC_{50-Lyase} = & -0.891\ (\pm 0.298) + 0.448\ (\pm 0.026) < 6 - integer > \\ & -1.028\ (\pm 0.137) indicator2 + 1.214 < 0.74 - \pi_m > \\ & +1.069\ (\pm 0.241) < 0.74 - \pi_m > \\ & -0.572\ (\pm 0.190) MR_p \end{aligned} \quad (2)$$

For the lyase inhibitory activity, the Integer value should be equal to or greater than 6 for optimal inhibitory activity (e.g., compounds **30**, **31**, and **38**). Compounds **11, 2, 10,** (integer value 1), compound **35** (integer value 3) showed poor inhibitory activity. I_{azole} indicates the type of azole ring connected to the phenyl ring. The value is 0 for triazole and 1 for imidazole. The positive contribution of the term I_{azole} indicates the imidazole ring favors the lyase inhibitory activity, corroborating the results that "imidazole compounds are more potent inhibitors than the triazole-based compounds" stated in the literature. L is a steric parameter, which is the length of the substituents along the axis of their substitution to the parent skeleton. The term <L_p-2.65> with a negative regression coefficient indicates that to avoid detrimental interactions, the value of L_p should be less than 2.65. L_p is the length of the substitutions at the 4 (*para*) position of the terminal phenyl ring. Compounds with high values of L_p, for example, **26, 32, 33,** showed better inhibitory activities than those (compounds **38, 39,** etc.) with a numerical value less than 2.65. The parameter π is the lipophilicity substitution constant, which is a very important parameter in modeling studies. The term <0.74–π_m> has a negative regression coefficient, indicating the value of π_m should be more than 0.74 for optimal activity. The lipophilic substitutions at the terminal phenyl ring are detrimental for the inhibitory activity. Only compounds **10** and **13** had a value greater than 0.74 with $–CF_3$ and –Cl substitution and showed activity in a moderate range due to the less <6-integer> value. Rest of the compounds are unsubstituted at the *meta* position of the terminal phenyl ring. Compounds **33, 26,** and **32** with a high value of MRp showed better inhibitory activity than compounds like **2** and **10** with lower *MRp* values. The structural alerts from model 2 for compound 30, 10, 1, 34, 31, 2, 16, and 35 are highlighted in Figure 1(B).

3.2. Modeling with topological descriptors

3.2.1. Hydroxylase topological

$$\begin{aligned} pIC_{50-OHase} = & -6.351(\pm 0.736) \\ & +\ 0.186\ (\pm 0.029) Zagreb \\ & -0.392\ (\pm 0.071) SC_{3P} \\ & +\ 1.303\ (\pm 0.096)\ <5.601 - \phi > \end{aligned} \quad (3)$$

The term <5.601-ϕ> with negative regression coefficient indicates that the value of molecular should be greater than 5.601. Compounds **27** and **33** (ϕ> 5.601) showed more significant inhibitory activity than compounds **8, 9, 10,** and **11** with lower ϕ values. It is obvious from the observations that molecular flexibility increases with an increase in the number of alkyl groups between the phenyl and azole rings (e.g., **33, 25, 27, 30, 29,** and **28**) as well as the introduction of additional ring system (**43, 46, 47,** and **49**). Zagreb which indicates the extent of branching of the molecular carbon atom skeleton has a detrimental effect on the inhibitory activity. Compounds like **1** (H), **2** (F), **8** (–CH3), and **10** (CF_3) showed lower Zagreb values and poor inhibitory activities. It was observed that compounds **25, 27, 28, 30, 33** have a higher Zagreb value, and they showed significantly higher activity. *SC_3P* is the number of paths of length 3 in the molecules and indicates the

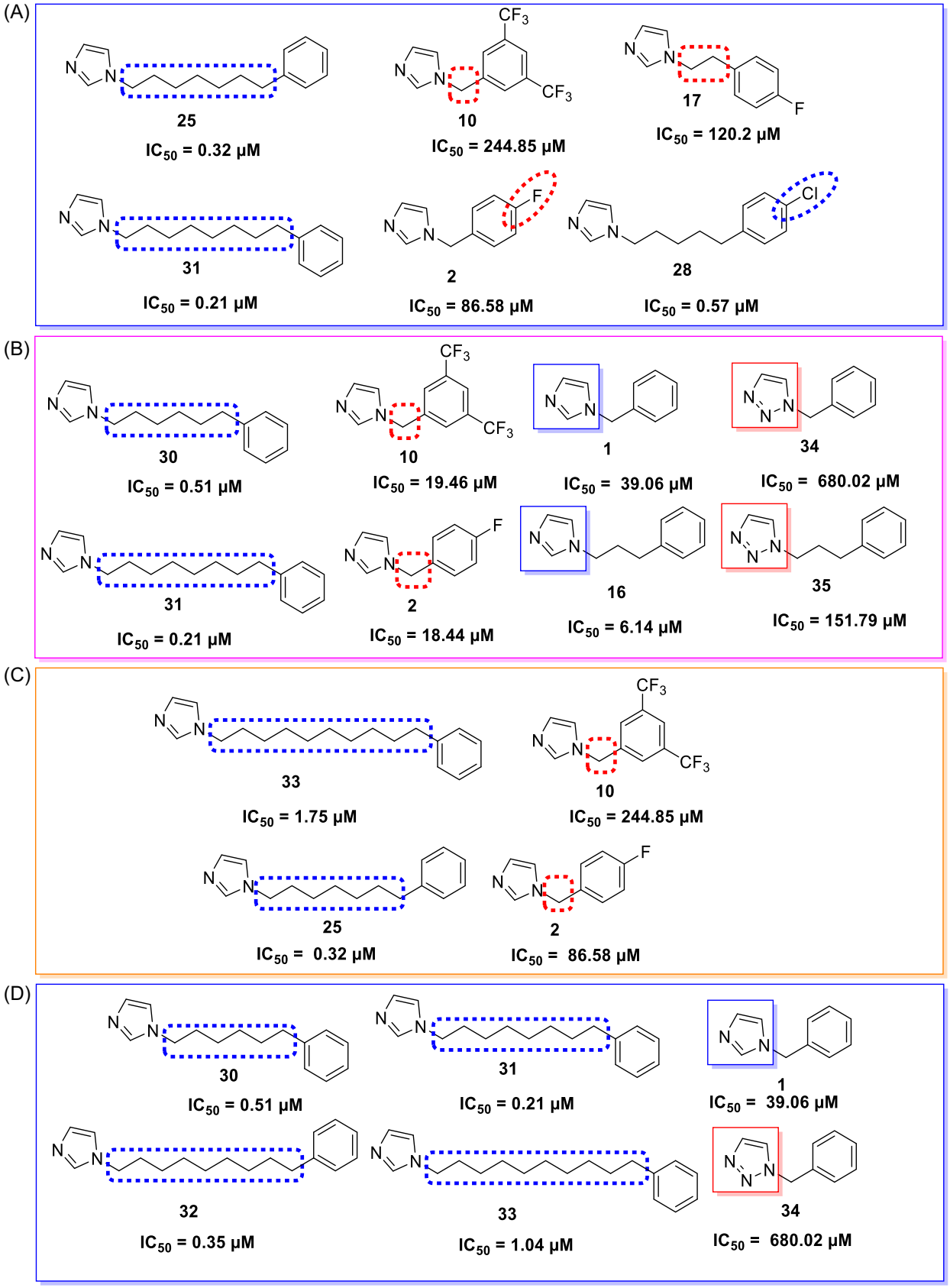

Figure 1. Structural alerts from (A) model 1, (B) model 2, (C) model 3, and (D) model 4

importance of linear branching in the structures that facilitates inhibitory activity. The structural alerts from model 3 for compounds 33, 10, 25, and 2 are highlighted in Figure 1(C).

3.2.2. Lyase topological

$$\begin{aligned} pIC_{50-Lyase} = & -10.677\ (\pm 1.132) \\ & +0.429\ (\pm 0.045) S\_aaCH \\ & +\ 3.932\ (\pm 0.388) JX \\ & -\ 0.415\ (\pm 0.050) S\_aaN \\ & -\ 0.629\ (\pm 0.085) S\_aasC \\ & +1.276\ (\pm 0.301)\ {}^{3}\chi_c^{v} \end{aligned} \quad (4)$$

JX reflects the relative connectivity and effective size of the carbon chain to which multiple methyl groups are attached. The presence of a higher number of alkyl groups increases the inhibitory activity (for compounds like **25, 27, 28**, **29, 31, 32,** and **33** with numbers of alkyl chains 7, 7, 5, 5, 8, 9, and 10, respectively) due to lower JX values. For compounds (like **44, 46**, and **47**) with an additional ring system, the value of JX decreases and increases the inhibitory activity. Third-order valance-modified cluster connectivity index ($^{3}\chi_c^{v}$) indicates the impact of branching and shows a favorable impact on the inhibition effects. Compounds **44, 46, 47, 48** with high values of above parameter showed more significant inhibitory activity than compounds **34** and **35**. The E-state index of fragments  (SaaCH) is detrimental for inhibitory activity, whereas the E-state index of fragments  (SaasC) and (SaaN) produce conducive activity. The fragment  present in the imidazole ring system and for triazole compounds (**34, 35, 36, 37, 39, 40,** and **42**) bears a value of zero. This indicates the importance of the imidazole ring for lyase inhibitory activity as observed for the compounds **25, 30, 29,** and **27** with a high value of the parameter. The structural alerts from model 4 for compounds 30, 31, 1, 32, 33, and 34 are highlighted in Figure 1(D).

3.3. Designing of novel CYP17 hydroxylase and lyase inhibitors

The novel CYP17 hydroxylase and lyase inhibitors were designed from the mechanistic interpretation of both Hansch and topological models (Equations (1), (2), (3), and (4)) substitution approach. In this regard, a primary aromatic ring X and imidazole ring Y are constant in all compounds. The intermediate connecting alkyl unit (linker) length was considered between the six to ten carbons. The *para* and *meta* positions of the aromatic X ring were substituted with different substituents to improve the potency. The details of the design strategy are shown in Figure 2. The combinatorial libraries of novel 3645 inhibitors were designed using SmiLib software.

3.4. Finding of novel and potential CYP17 hydroxylase inhibitors

In regard to finding the potential CYP17 hydroxylase inhibitors, all the designed 3645 compounds were screened on model or Equation (3) to estimate the inhibitory activity. Among these, 3065 compounds showed IC_{50} lower than 10 µM, 1578 are having IC_{50} below 1 µM and just 59 are showing more than 100 µM. When we applied the HAT value cut-off, we got 2630 compounds with IC_{50} less than 6 µM. Additionally, we filtered these compounds and prioritized eleven novel compounds having IC_{50} value less than 0.17 µM (the most potent compound in the dataset). The structures of these potential hits were reported in Table S4. The docking validation was performed, and it is in accepted range. Co-crystal superimposition was showed in Figure S3. Further, these eleven compounds, KTZ, and co-crystal were docked on CYP17 hydroxylase target (PDB ID: 3ruk) to find molecular mechanism, binding affinity, and interaction pattern of novel inhibitors. The docking score, Fe-N distance, IC_{50} values, and different residues involved in forming favorable interactions are given in Table 2. All the docked compounds have showed docking score ranges between 116.44 and 137.59. The compound 401 showed the highest docking score of 137.59 and had IC_{50} 0.144 µM. A total of five compounds (81, 369, 401, 441, and 473) showed a higher docking score (133.31, 133.05, 137.59, 136.34, and 130.77, respectively) than that of standard KTZ (129.54), co-crystal (126.88), and the most potent compound L27 of the dataset (123.38). Along with the docking score, we observed that the heme coordination and the distance between the heme and heterocyclic atom (nitrogen or oxygen) also play an important role in improving hydroxylase inhibitory potential [32]. The most potent compounds 81, 369, 401, 441, and 473 showed Fe-N distances of 2.50, 2.32, 2.28, 2.42, and 2.34 Å, respectively, while KTZ (4.15 Å), co-crystal (2.42 Å), and most potent compound L27 of the dataset (2.53 Å). The closer the distance between heme and nitrogen will have better the inhibitory activity due to coordination with iron. Along with the Fe-N distance, similar fact was found for oxygen-containing compounds like compounds 196, 441, and co-crystal. The common favorable amino acid interaction includes hydrogen bond, hydrophobic, and halogen interactions. The ALA367, ALA302, HEM600, ALA113, PHE114, CYS442, ILE205, ILE206, VAL482, VAL483, ASP298, GLY297, VAL366, TYR201, and ARG239

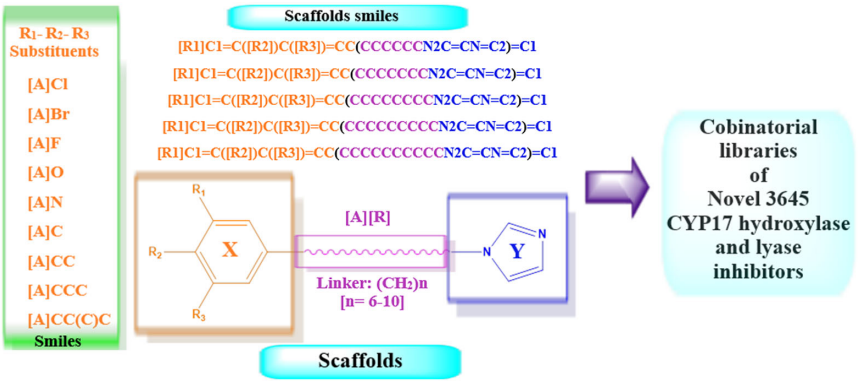

Figure 2. Design parameters, smiles, and design scaffolds

Table 2. The docking score, Fe-N distance, IC_{50} values, and different residues involved in forming favorable interactions of novel hydroxylase inhibitors

Name of compounds	LibDock Score	Distance Fe-N (Å)	IC_{50} (μM)	Favorable interactions forming residues
52	116.44	2.47	0.122	ALA367, **ALA302**, HEM600, ALA113, VAL236, ILE205, ARG239, TYR201, PHE114
73	124.36	2.34	0.144	ALA367, ALA302, HEM600, ALA113, ILE205
81	133.31	2.50	0.144	ALA367, ALA302, HEM600, ALA113, ILE206, CYS442, VAL482, VAL483, VAL366
153	126.88	2.36	0.148	ALA367, ALA302, HEM600, ALA113, PHE114, ILE206, VAL482, VAL483, GLY301, ILE371
196	125.24	2.41, **2.02**	0.122	**ASN202**, ALA367, ALA302, HEM600, ALA113, PHE114, ILE371, ILE205
212	121.40	2.43	0.122	**ASN202**, ALA367, ALA302, HEM600, ALA113, ILE205, **GLY301**, TYR201, GLY297
361	121.49	2.30	0.144	ALA367, ALA302, HEM600, VAL482, VAL483, GLY301, **ASP298, GLY297, VAL366**
369	133.05	2.32	0.148	ALA367, ALA302, HEM600, CYS442, ILE205, ILE206, VAL482, VAL483, GLY301, **ASP298, GLY297, VAL366**
401	137.59	2.28	0.144	ALA367, **ALA302**, HEM600, ILE206, ILE205, ARG239, TYR201, **ASP298**, GLY297
441	136.34	2.42, **2.26**	0.144	ALA367, ALA302, HEM600, ALA113, ILE205, ILE206, GLY301, PHE114, **ASN202**, VAL483, ILE371
473	130.77	2.34	0.144	ALA367, ALA302, HEM600, CYS442, ILE205, ILE206, VAL482, VAL483,**ASP298, GLY297, VAL366,** TYR201
L27	123.38	2.53	0.17	ALA367, ALA302, HEM600, ILE205, ALA113, PHE114, ASN202
KTZ	129.54	4.15, 8.60	3.76	ALA367, ALA302, HEM600, ILE206, TYR201, PHE300, ARG239, LEU243
Redocked Co-crystal	126.88	2.42, **2.07**	NA	ALA367, ALA302, HEM600, ILE205, ILE206, VAL482, VAL483, VAL366

Note: The values in bold in column number three are for the Fe-O distance.

residue interactions are important for the inhibitory action. The 2D and 3D interactions for all the potential compounds were shown in supplementary Figures 1–26.

Followed by docking analysis, binding energy calculations were performed for the eleven hit compounds. The details of the different energy parameters obtained by binding energy calculations are reported in Table 3. All the subjected compounds showed good binding affinity towards the targeted protein. Here, based on binding free energy, we identified four potential inhibitors (361, 369, 401, and 441) that showed BE more than −130 Kcal/mol. The compound 369 showed the highest BE (−137.43 Kcal/mol), which is more than co-crystal BE (−135.22 Kcal/mol).

Finally, we identified six potential inhibitors, both having docking scores greater than 130 or binding free energy more than −130 Kcal/mol and IC_{50} better than standards. Among these six compounds (Figure 3), 369 have the highest BE (−137.43 Kcal/mol) and 133.05 docking score. It showed four hydrogen bond interactions with GLY297, ASP298, and VAL366 and eleven hydrophobic interactions with ALA367,

Table 3. The different energy parameters obtained by binding energy calculation for novel hydroxylase inhibitors

Name	Binding energy	Ligand energy	Protein energy	Complex energy	Ligand Conf. energy
52	−102.47	17.91	−28956.9	−29041.5	7.33
73	−83.52	22.57	−28956.9	−29017.9	3.93
81	−115.88	39.64	−28956.9	−29033.2	5.15
153	−81.90	31.08	−28956.9	−29007.8	8.76
196	−122.45	30.77	−28956.9	−29048.6	9.73
212	−112.98	13.96	−28956.9	−29055.9	6.46
361	−132.59	5.17	−28956.9	−29084.4	6.47
369	−137.43	1.02	−28956.9	−29093.3	5.69
401	−130.72	19.57	−28956.9	−29068.1	5.75
441	−134.80	29.98	−28956.9	−29061.8	8.71
473	−120.01	9.99	−28956.9	−29066.9	5.16
Co-crystal	−135.22	122.47	−28956.9	−28969.7	0.06
KTZ	−145.39	51.31	−28956.9	−29051	12.45

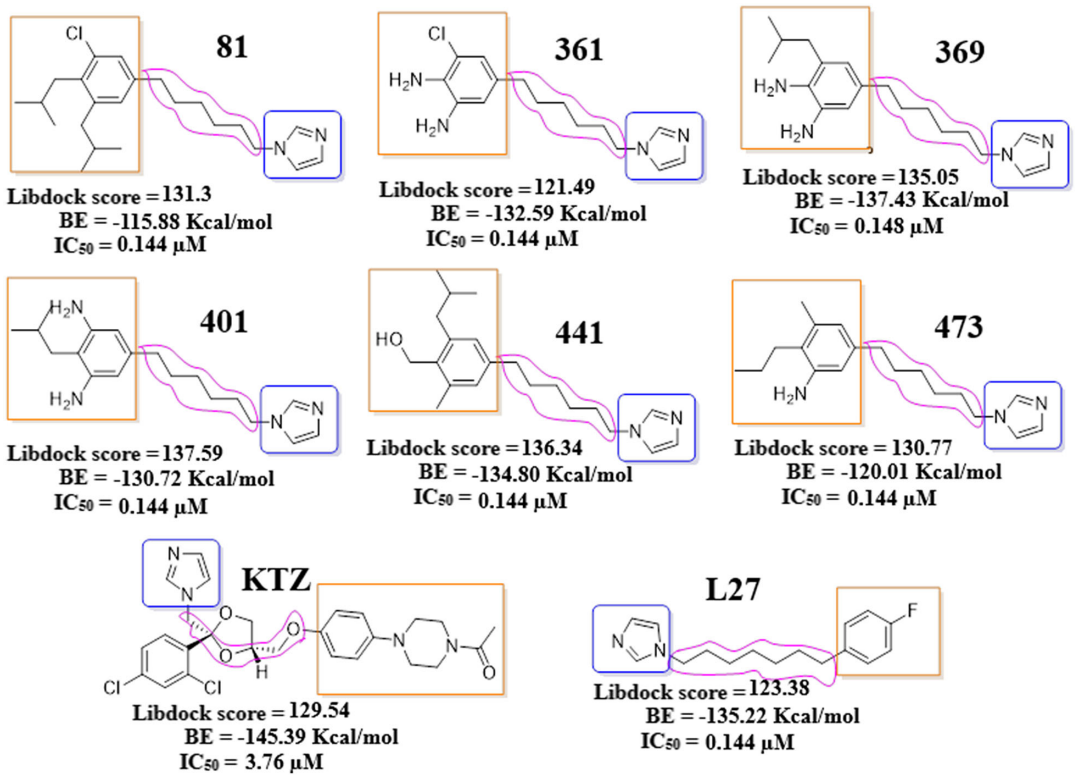

Figure 3. The six novel potential hydroxylase inhibitors (compound 81, 361, 369, 401, 441, and 473) and standards

ALA302, HEM600, CYS442, ILE205, ILE206, VAL482, VAL483, and GLY301. The Fe-N distance was found to be 2.32 Å, and it is better than the standard and co-crystal. The 2D and 3D interactions of compound 369 are shown in Figure 4(A). Additionally, the ADME properties and toxicity profiling of these six hit compounds were carried out using DSC 4.1. The results suggested all the compounds having drug-like properties and are non-toxic in nature (Non-mutagenic, Non-carcinogenic, High LD_{50}, non-hepatotoxic, etc.). The results were reported in Tables S6 and S7 in supporting information 3.

3.5. Finding of novel and potential CYP17 lyase inhibitors

In regard to finding the potential CYP17 lyase inhibitors, all the designed 3645 compounds were screened on model 4 to estimate the lyase inhibitory activity. All 3645 compounds showed IC_{50} lower than 6 µM. We filtered these compounds by applying the HAT value cut-off (0.5000) and IC_{50} cut-off (0.056 µM) of the most potent compound in the dataset (L27), and we got seventeen compounds with IC_{50} ranges between 0.033 and 0.006 µM. The structures of these potential hits were reported in Table S5. Further, these seventeen compounds and standard drugs (KTZ and co-crystal) were docked on CYP17 lyase target (PDB ID: 3ruk) to find molecular mechanism, binding affinity, and interaction pattern of novel inhibitors. The docking score, Fe-N distance, IC_{50} values, and different residues involved in forming favorable interactions are given in Table 4.

All seventeen compounds showed strong docking score ranges between 119.66 and 135.86, while the nine compounds showed a higher docking score than standards. The compound 301 showed highest docking score of 135.86 and had IC_{50} 0.013 µM. The compounds 229, 238, 301, 302, 305, 309, 318, 382, and 625 showed higher docking score of 129.65, 131.78, 135.16, 133.65, 135.15, 129.65, 131.78, 133.65, and 135.65 respectively than those of standard KTZ (129.54), co-crystal (126.88), and the most potent compound L27 of the dataset (123.38).

Similar to the hydroxylase inhibitor pattern, here also heme coordination and the distance between heme and heterocyclic atom (nitrogen or oxygen) play an important role in improving lyase inhibitory action. The most potent compounds 229, 238, 301, 302, 305, 309, 318, 382, and 625 showed Fe-N distances of 2.36, 2.40, 2.41, 2.74, 2.40, 2.36, 2.32, 2.74, and 2.22 Å, respectively, while KTZ, co-crystal, and most potent compound L27 of the dataset showed 4.15, 2.42, and 2.53 Å, respectively. Among these nine compounds, six compounds have OH group, and the oxygen forms better coordination with heme, improving their potential. The Fe-O distance for oxygen-containing compounds like compounds 238, 301, 305, 309, 318, and 625 was found to be 2.19, 2.20, 2.25, 2.18, 2.19, and 2.05 Å, respectively. The similar favorable interactions like hydrogen bond, hydrophobic, and halogen interactions were found for lyase inhibitors as they are found for hydroxylase inhibitors with ALA367, ALA302, HEM600, ALA113, PHE114, CYS442, ILE205, ILE206, VAL482, VAL483, ASP298, GLY297, VAL366, TYR201, and ARG239 residues. The 2D and 3D interactions for all the potential compounds were shown in supplementary Figures 1–26.

Similar to hydroxylase inhibitors, binding energy calculations were also performed for the potential seventeen compounds. The details of the different energy parameters obtained by binding energy calculations are reported in Table 5. All the subjected compounds showed strong binding affinity towards the targeted protein. All the potential inhibitors obtained by docking showed

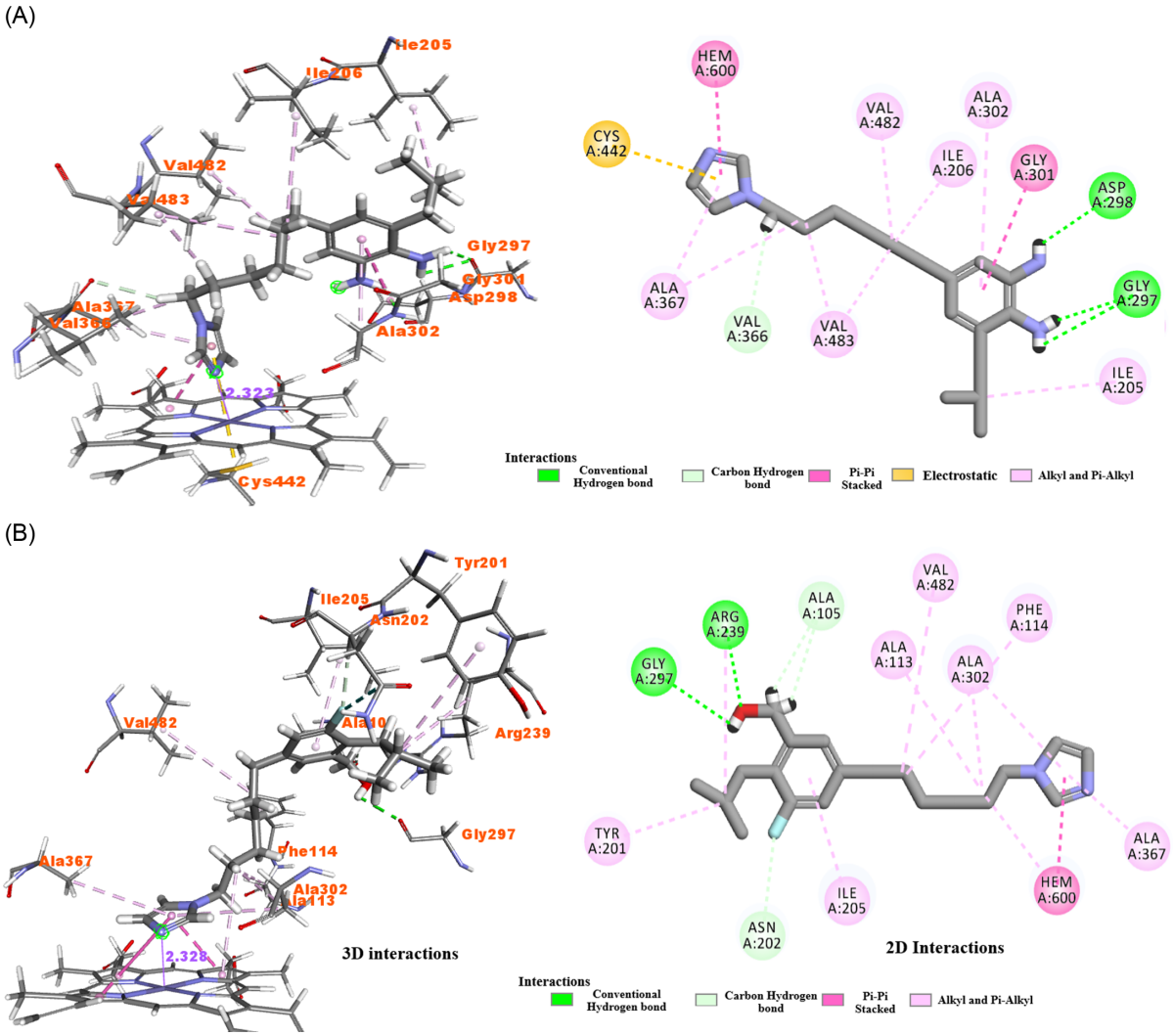

Figure 4. 2D and 3D interactions of the most promising hydroxylase inhibitor (compound 369) (A) and lyase inhibitor (compound 318) (B) within the active pocket of 3ruk protein

BE more than −130 Kcal/mol, while the compounds 238, 301, 318, and 625 showed −158.80, 152.45, −158.88, and −148.18 Kcal/mol, respectively, which is far higher than standard or co-crystal.

Finally, we identified nine potential inhibitors which both having a docking score of more than 130 or binding free energy of more than −130 Kcal/mol and IC_{50} better than standards, which are shown in Figure 5. Among these nine compounds, 318 have the highest BE (−158.88 Kcal/mol) and 131.78 docking score. It showed favorable interactions with ALA367, ALA302, HEM600, ALA113, ILE205, **ARG239**, TYR201, PHE114, **ASN202**, **GLY297**, **ALA105,** and VAL482 residues. The residues highlighted in bold showed the hydrogen bond interactions. The Fe-N and Fe-O distances in the two best poses for 318 were found to be 2.32 and 2.19 Å, respectively. The 2D and 3D interactions of compound 318 are shown in Figure 4(B). Additionally, the ADME properties and toxicity profiling of these nine hit compounds was performed. The results suggested all the compounds have drug-like properties and being non-toxic in nature (non-mutagenic, non-carcinogenic, high $LD_{50,}$ non-hepatotoxic, etc.). The results were reported in Tables S8 and S9 in supporting information 3.

3.6. Study of most potent and selective inhibitor 625

The best and most potent compound from the designed novel inhibitors was found to be compound 625 having lyase inhibitory activity with IC_{50} 0.006 µM. It is a selective lyase inhibitor (375-fold more selective) but also showed a good IC_{50} value (2.253 µM) against the hydroxylase. The structural features consist of a basic imidazole and phenyl ring connected with six carbon alkyl chains. The *meta* position of the phenyl ring was substituted with -CH_2-OH- and the propyl group while the *para* position was substituted with the ethyl group. The substitutional effect was clearly observed in the sense of IC_{50} as well as the docking interactions and scores. Compound 625 showed twelve favorable interactions with ALA367, ALA302, HEM600, ILE205, ALA113, **ASP298, GLY297, ALA105, ARG239,** CYS442 residues. From this, para and meta substituents showed six favorable interactions and remaining six interactions were showed by whole scaffold. The LibDock score, Fe-N distance, and the BE was found to be 135.15, 2.22 Å, and 148.18 Kcal/mol, which is far better than the standard co-crystal or abiraterone.

Table 4. The docking score, Fe-N distance, IC_{50} values, and different residues involved in forming favorable interactions of novel lyase inhibitors

Name of compounds	LibDock score	Distance Fe-N (Å)	IC_{50} (μM)	Favorable interactions forming residues
223	121.57	2.63	0.029	**ASN202**, ALA367, ALA302, HEM600, ALA113, PHE114, ILE205
224	125.75	2.40	0.033	ALA367, ALA302, HEM600, ALA113, PHE114, ILE371, ILE205, ALA105
229	129.65	2.36	0.009	ALA367, ALA302, HEM600, ALA113, ILE371, ALA105, GLY297
238	131.78	2.40, **2.19**	0.008	ALA367, **ALA302**, HEM600, ALA113, ILE205, ARG239, PHE114, VAL482, **ASN202**, TYR201, **ASP298**, **ALA105**
255	119.66	2.43	0.017	ALA367, **ALA302**, HEM600, ALA113, ILE205, ARG239, TYR201, PHE114, ASN202, **ASP298**, **ALA105, GLY297**
264	126.96	2.33	0.018	ALA367, ALA302, HEM600, ALA113, **ARG239**, PHE114, **ASN202**, **ASP298**, **GLY297,** ILE371, GLY301
301	135.86	2.41, **2.20**	0.013	ALA367, ALA302, HEM600, ALA113, ILE205, **ARG239**, **TYR201**, PHE114, **ASN202**, **ASP298**, **ALA105,** ILE371
302	133.65	2.74	0.010	ALA367, ALA302, HEM600, ALA113, ILE205, ARG239, PHE114, **ALA105,**
305	135.15	2.4, **2.25**	0.006	ALA367, ALA302, HEM600, ALA113, ILE205,PHE114, **GLY297,** VAL483, ILE206, ILE371
309	129.65	2.36, **2.18**	0.009	ALA367, ALA302, HEM600, ALA113, GLY297, ILE371, ALA105
318	131.78	2.32, **2.19**	0.007	ALA367, ALA302, HEM600, ALA113, ILE205, **ARG239**, TYR201, PHE114, **ASN202**, **GLY297**, **ALA105,** VAL482
382	133.65	2.74	0.010	ALA367, ALA302, HEM600, ALA113, ILE205, ARG239, PHE114, **ALA105**
383	120.89	2.37	0.008	ALA367, HEM600, CYS442, ILE205, ILE206, VAL482, VAL483, **ASP298, GLY297, VAL366, ASN202**
543	121.57	2.63	0.028	ALA367, ALA302, HEM600, ALA113, ILE205, PHE114, ASN202
624	125.75	2.42	0.033	ALA367, ALA302, HEM600, ALA113, ILE205, PHE114, ILE206, ILE371
625	135.15	2.22, **2.03**	0.006	ALA367, ALA302, HEM600, ILE205, ALA113, **ASP298, GLY297, ALA105, ARG239,**CYS442
953	129.39	2.42	0.019	ALA367, ALA302, HEM600, CYS442, ILE205, ILE206, VAL482, VAL483, ALA105, ASP298, TYR201
KTZ	129.54	4.15, 8.60	1.66	ALA367, ALA302, HEM600, ILE206, TYR201, PHE300, ARG239, LEU243
L27	123.38	2.53	0.056	ALA367, ALA302, HEM600, ILE205, ALA113, PHE114, ASN202
Bound Co-crystal	NA	2.22	NA	ALA367, ALA302, HEM600, ILE205, ILE206, VAL482, ALA113, PHE114, TYR201

Note: The values in bold in column number three are for the Fe-O distance.

Table 5. The different energy parameters obtained by binding energy calculation for novel lyase inhibitors

Name	Binding energy	Ligand energy	Protein energy	Complex energy	Ligand Conf. energy
223	−106.22	17.11	−28956.9	−29046	2.60
229	−120.03	31.97	−28956.9	−29045	6.74
238	−158.80	27.77	−28956.9	−29088	5.41
255	−123.54	22.77	−28956.9	−29057.7	6.35
264	−122.11	22.85	−28956.9	−29056.2	2.44
301	−152.45	21.14	−28956.9	−29088.2	9.52
302	−137.78	16.90	−28956.9	−29077.8	4.28
305	−138.17	24.36	−28956.9	−29070.7	3.34
309	−119.39	17.38	−28956.9	−29058.9	5.93
318	−158.88	27.78	−28956.9	−29088	5.39
382	−137.77	16.91	−28956.9	−29077.8	4.28
383	−120.32	9.92	−28956.9	−29067.3	4.16
393	−120.01	9.99	−28956.9	−29066.9	5.16
543	−106.23	17.10	−28956.9	−29046.1	2.63
624	−92.88	20.63	−28956.9	−29029.2	5.26
625	−148.18	24.39	−28956.9	−29070.7	3.34
953	−108.21	22.03	−28956.9	−29043.1	4.95
Co-crystal	−135.22	122.47	−28956.9	−28969.7	0.06
KTZ	−145.39	51.31	−28956.9	−29051	12.45

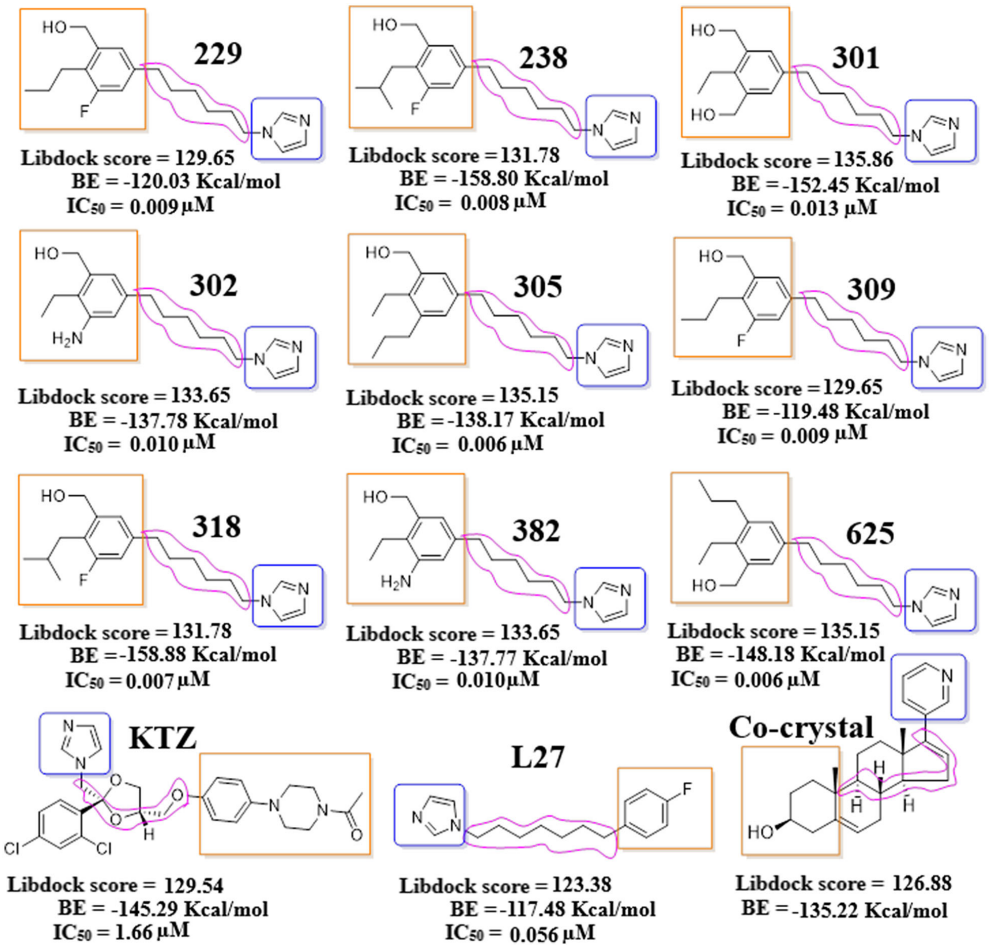

Figure 5. The nine-novel potential lyase inhibitors (compound 229, 238, 301, 302, 305, 309, 318, 382, and 625) and standards

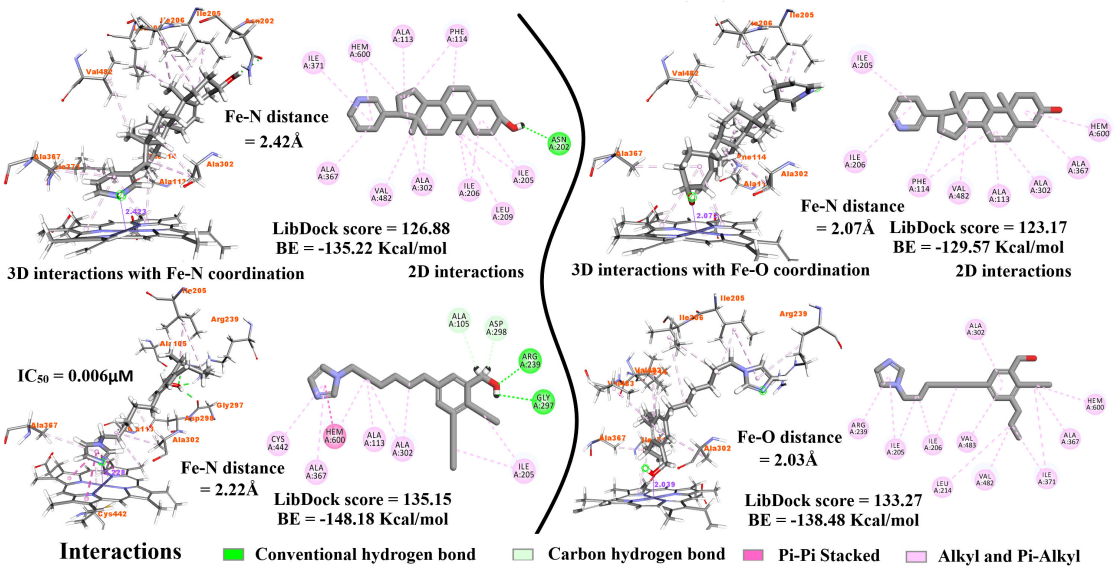

Figure 6. 2D and 3D interactions of most potent 625 and selective lyase inhibitor and co-crystal (abiraterone) within the active pocket of 3ruk

Surprisingly, we found that the oxygen atom (both in 625 and abiraterone) also forms a coordination with the heme moiety. The second-best pose in both the 625 and abiraterone showed heme coordination (Fe-O) with lesser distance (2.03 and 20.7 Å respectively) than that of Fe-N [36]. The favorable interactions are also similar to those of best pose and the co-crystal interactions. The 2D and 3D interactions and distances (Fe-N, Fe-O) for compound 625 and abiraterone are shown in Figure 6.

4. Conclusion

The study used the Hansch approach and docking insights to design CYP17 inhibitors based on substitution effects. Initially, the two best predictive and statistically robust QSAR models were developed for the azole-containing CYP17 hydroxylase and lyase inhibitors. Hansch and topological-based models were able to identify and study the substitution effect and the actual contribution of topological parameters to get a potential inhibitory response. The developed models state that the length of alkyl substitution is essential for optimal activity (7 or more for hydroxylase and 6 or more for lyase) and the imidazole ring is more promising for lyase inhibitory activity. The *para* and *meta* position substitutions (OH, Cl, F, Br, -CH_2-OH, methyl, ethyl, propyl, isopropyl) on the phenyl ring influence the inhibitory activity. Based on these observations, we designed and screened a combinatorial library of 3645 compounds over the topological model to get predicted IC_{50}. Further, the compounds were filtered by means of the HAT cut-off, predicted IC_{50}, and docking scores. The BE calculations were performed to get binding affinity, interactions, and binding patterns towards the hydroxylase and lyase proteins. Additionally, ADME and toxicity profiling were performed to get drug-like and non-toxic, or less toxic compounds. From this study, we found that the compounds 369 and 318 were found to be potential hydroxylase and lyase inhibitors, respectively. The compound 625 is found to be the most potent and selective lyase inhibitor. These drug-like compounds could be useful in prostate cancer chemotherapy.

Acknowledgement

The authors acknowledge Prof. Paola Gramatica for the free license of QSARINS. One of the authors BWM thanks to Mahatma Jyotiba Phule Research & Training Institute (MAHAJYOTI), Nagpur, Government of Maharashtra for financial assistance in the form of MJPRF-22 Ph.D. Fellowship. One of the authors AM thanks to Ministry of Tribal Affairs, Government of India for financial assistance in the form Ph.D. Fellowship.

Conflicts of Interest

The authors declare that they have no conflicts of interest to this work.

Data Availability Statement

The data that support this work are available upon reasonable request to the corresponding author.

Author Contribution Statement

Balaji Wamanrao Matore: Data curation, Writing – original draft, Visualization. **Anjali Murmu:** Writing – review & editing. **Jagadish Singh:** Formal analysis, Investigation. **Partha Pratim Roy:** Conceptualization, Methodology, Software, Validation, Resources, Supervision, Project administration.

Supplementary Information

The supplementary file is available at https://doi.org/10.47852bonviewMEDIN52024158.

References

[1] Siegel, R. L., Miller, K. D., Funchs, H. E., & Jemal, A. (2022). Cancer statistics, 2022. *CA: A Cancer Journal for Clinicians*, *72*(1), 7–33. https://doi.org/10.3322/caac.21708

[2] Rawla, P. (2019). Epidemiology of prostate cancer. *World Journal of Oncology*, *10*(2), 63–89. https://doi.org/10.14740/wjon1191

[3] Dhawale, S. A., Bhosle, P., Mahajan, S., Patil, G., Gawale, S., Ghodke, M., . . . , & Ansari, A. (2024). Dual targeting in prostate cancer with phytoconstituents as a potent lead: A computational approach for novel drug discovery. *Journal of Biomolecular Structure and Dynamics*, *42*(17), 8906–8919. https://doi.org/10.1080/07391102.2023.2251059

[4] Latysheva, A. S., Zolottsev, V. A., Veselovsky, A. V., Scherbakov, K. A., Morozevich, G. E., Zhdanov, D. D., . . . , & Misharin, A. Y. (2023). Oxazolinyl derivatives of androst-16-ene as inhibitors of CYP17A1 activity and prostate carcinoma cells proliferation: Effects of substituents in oxazolinyl moiety. *The Journal of Steroid Biochemistry and Molecular Biology*, *230*, 106280. https://doi.org/10.1016/j.jsbmb.2023.106280

[5] Akhtar, M. K., Kelly, S. L., & Kaderbhai, M. A. (2005). Cytochrome b_5 modulation of 17α hydroxylase and 17–20 lyase (CYP17) activities in steroidogenesis. *Journal of Endocrinology*, *187*(2), 267–274. https://doi.org/10.1677/joe.1.06375

[6] Kolar, N. W., Swart, A. C., Mason, J. I., & Swart, P. (2007). Functional expression and characterisation of human cytochrome P45017α in *Pichia pastoris*. *Journal of Biotechnology*, *129*(4), 635–644. https://doi.org/10.1016/j.jbiotec.2007.02.003

[7] Ayub, M., & Levell, M. J. (1987). Inhibition of testicular 17α-hydroxylase and 17, 20-lyase but not 3β-hydroxysteroid dehydrogenase-isomerase or 17β-hydroxysteroidoxidoreductase by ketoconazole and other imidazole drugs. *Journal of Steroid Biochemistry*, *28*(5), 521–531. https://doi.org/10.1016/0022-4731(87)90511-5

[8] Kim, D., Kim, V., McCarty, K. D., & Guengerich, F. P. (2021). Tight binding of cytochrome b_5 to cytochrome P450 17A1 is a critical feature of stimulation of C21 steroid lyase activity and androgen synthesis. *Journal of Biological Chemistry*, *296*, 100571. https://doi.org/10.1016/j.jbc.2021.100571

[9] Vasaitis, T. S., Bruno, R. D., & Njar, V. C. O. (2011). CYP17 inhibitors for prostate cancer therapy. *The Journal of Steroid Biochemistry and Molecular Biology*, *125*(1–2), 23–31. https://doi.org/10.1016/j.jsbmb.2010.11.005

[10] Alex, A. B., Pal, S. K., & Agarwal, N. (2016). CYP17 inhibitors in prostate cancer: Latest evidence and clinical potential. *Therapeutic Advances in Medical Oncology*, *8*(4), 267–275. https://doi.org/10.1177/1758834016642370

[11] Reid, A. H. M., Attard, G., Barrie, E., & de Bono, J. S. (2008). CYP17 inhibition as a hormonal strategy for prostate cancer. *Nature Clinical Practice Urology*, *5*(11), 610–620. https://doi.org/10.1038/ncpuro1237

[12] Trachtenberg, J., Halpern, N., & Pont, A. (1983). Ketoconazole: A novel and rapid treatment for advanced prostatic cancer. *The Journal of Urology*, *130*(1), 152–153. https://doi.org/10.1016/S0022-5347(17)51007-1

[13] Wei, Z., Chen, C., Li, B., Li, Y., & Gu, H. (2021). Efficacy and safety of abiraterone acetate and enzalutamide for the treatment of metastatic castration-resistant prostate cancer: A systematic review and meta-analysis. *Frontiers in Oncology*, *11*, 732599. https://doi.org/10.3389/fonc.2021.732599

[14] Agarwal, N., Tangen, C. M., Hussain, M. H. A., Gupta, S., Plets, M., Lara, P. N., . . . , & Quinn, D. I. (2022). Orteronel

for metastatic hormone-sensitive prostate cancer: A multicenter, randomized, open-label phase III trial (SWOG-1216). *Journal of Clinical Oncology*, *40*(28), 3301–3309. https://doi.org/10.1200/JCO.21.02517

[15] Kwegyir-Afful, A. K., Ramalingam, S., Ramamurthy, V. P., Purushottamachar, P., Murigi, F. N., Vasaitis, T. S., …, & Njar, V. C. O. (2019). Galeterone and the next generation galeterone analogs, VNPP414 and VNPP433-3β exert potent therapeutic effects in castration-/drug-resistant prostate cancer preclinical models in vitro and in vivo. *Cancers*, *11*(11), 1637. https://doi.org/10.3390/cancers11111637

[16] Wróbel, T. M., Rogova, O., Sharma, K., Rojas Velazquez, M. N., Pandey, A. V., Jørgensen, F. S., …, & Björkling, F. (2022). Synthesis and structure–activity relationships of novel non-steroidal CYP17A1 inhibitors as potential prostate cancer agents. *Biomolecules*, *12*(2), 165. https://doi.org/10.3390/biom12020165

[17] Bennani, F. E., Karrouchi, K., Doudach, L., Scrima, M., Rahman, N., Rastrelli, L., …, & Ansar, M. (2022). In silico identification of promising new pyrazole derivative-based small molecules for modulating CRMP2, C-RAF, CYP17, VEGFR, C-KIT, and HDAC—Application towards cancer therapeutics. *Current Issues in Molecular Biology*, *44*(11), 5312–5351. https://doi.org/10.3390/cimb44110361

[18] Rudovich, A. S., Peřina, M., Krech, A. V., Novozhilova, M. Y., Tumilovich, A. M., Shkel, T. V., …, & Khripach, V. A. (2022). Synthesis and biologicale evaluation of new isoxazolyl steroids as anti-prostate cancer agents. *International Journal of Molecular Sciences*, *23*(21), 13534. https://doi.org/10.3390/ijms232113534

[19] Wróbel, T. M., Jørgensen, F. S., Pandey, A. V., Grudzińska, A., Sharma, K., Yakubu, J., & Björkling, F. (2023). Non-steroidal CYP17A1 inhibitors: Discovery and assessment. *Journal of Medicinal Chemistry*, *66*(10), 6542–6566. https://doi.org/10.1021/acs.jmedchem.3c00442

[20] Bonomo, S., Hansen, C. H., Petrunak, E. M., Scott, E. E., Styrishave, B., Jørgensen, F. S., & Olsen, L. (2016). Promising tools in prostate cancer research: Selective non-steroidal cytochrome P450 17A1 inhibitors. *Scientific Reports*, *6*(1), 29468. https://doi.org/10.1038/srep29468

[21] Matore, B. W., Banjare, P., Sarthi, A. S., Roy, P. P., & Singh, J. (2023). Phthalimides represent a promising scaffold for multi-targeted anticancer agents. *ChemistrySelect*, *8*(9), e202204851. https://doi.org/10.1002/slct.202204851

[22] Murmu, A., Banjare, P., Matore, B. W., Roy, P. P., & Singh, J. (2024). 1, 3, 4-oxadiazole: An emerging scaffold to inhibit the thymidine phosphorylase as an anticancer agent. *Current Medicinal Chemistry*, *31*(38), 6227–6250. https://doi.org/10.2174/0929867331666230712113943

[23] Hossain, M., Habib, I., Singha, K., & Kumar, A. (2024). FDA-approved heterocyclic molecules for cancer treatment: Synthesis, dosage, mechanism of action and their adverse effect. *Heliyon*, *10*(1), e23172. https://doi.org/10.1016/j.heliyon.2023.e23172

[24] Kumar, A., Singh, A. K., Singh, H., Vijayan, V., Kumar, D., Naik, J., …, & Kumar, P. (2023). Nitrogen containing heterocycles as anticancer agents: A medicinal chemistry perspective. *Pharmaceuticals*, *16*(2), 299. https://doi.org/10.3390/ph16020299

[25] Bird, I. M., & Abbott, D. H. (2016). The hunt for a selective 17, 20 lyase inhibitor; learning lessons from nature. *The Journal of Steroid Biochemistry and Molecular Biology*, *163*, 136–146. https://doi.org/10.1016/j.jsbmb.2016.04.021

[26] Rafferty, S. W., Eisner, J. R., Moore, W. R., Schotzinger, R. J., & Hoekstra, W. J. (2014). Highly-selective 4-(1, 2, 3-triazole)-based P450c17a 17, 20-lyase inhibitors. *Bioorganic & Medicinal Chemistry Letters*, *24*(11), 2444–2447. https://doi.org/10.1016/j.bmcl.2014.04.024

[27] Carradori, S., Ammazzalorso, A., de Filippis, B., Şahin, A. F., Akdemir, A., Orekhova, A., …, & Simonetti, G. (2022). Azole-based compounds that are active against *Candida* biofilm: In vitro, in vivo and in silico studies. *Antibiotics*, *11*(10), 1375. https://doi.org/10.3390/antibiotics11101375

[28] Khalil, N. A., Ahmed, E. M., Zaher, A. F., Sobh, E. A., El-Sebaey, S. A., & El-Zoghbi, M. S. (2021). New benzothieno [2, 3-*c*] pyridines as non-steroidal CYP17 inhibitors: Design, synthesis, anticancer screening, apoptosis induction, and *in silico* ADME profile studies. *Journal of Enzyme Inhibition and Medicinal Chemistry*, *36*(1), 1839–1859. https://doi.org/10.1080/14756366.2021.1958212

[29] Padmakar Darne, C., Velaparthi, U., Saulnier, M., Frennesson, D., Liu, P., Huang, A., …, & Balog, A. (2022). The discovery of BMS-737 as a potent, CYP17 lyase-selective inhibitor for the treatment of castration-resistant prostate cancer. *Bioorganic & Medicinal Chemistry Letters*, *75*, 128951. https://doi.org/10.1016/j.bmcl.2022.128951

[30] Ajduković, J. J., Djurendić, E. A., Petri, E. T., Klisurić, O. R., Ćelić, A. S., Sakač, M. N., …, & Penov Gaši, K. M. (2013). 17 (*E*)-picolinylideneandrostane derivatives as potential inhibitors of prostate cancer cell growth: Antiproliferative activity and molecular docking studies. *Bioorganic & Medicinal Chemistry*, *21*(23), 7257–7266. https://doi.org/10.1016/j.bmc.2013.09.063

[31] Matore, B. W., Banjare, P., Singh, J., & Roy, P. P. (2022). *In silico* selectivity modeling of pyridine and pyrimidine based CYP11B1 and CYP11B2 inhibitors: A case study. *Journal of Molecular Graphics and Modelling*, *116*, 108238. https://doi.org/10.1016/j.jmgm.2022.108238

[32] McSkimming, A., & Thompson, N. B. (2022). Four-coordinate Fe N_2 and imido complexes supported by a hemilabile NNC heteroscorpionate ligand. *Inorganic Chemistry*, *61*(31), 12318–12326. https://doi.org/10.1021/acs.inorgchem.2c01656

[33] Sohail, M., Bilal, M., Maqbool, T., Rasool, N., Ammar, M., Mahmood, S., …, & Ashraf, G. A. (2022). Iron-catalyzed synthesis of *N*-heterocycles via intermolecular and intramolecular cyclization reactions: A review. *Arabian Journal of Chemistry*, *15*(9), 104095. https://doi.org/10.1016/j.arabjc.2022.104095

[34] Song, D., Zhang, J., Wang, Y., Hu, J., Xu, S., Xu, Y., …, & Sun, Z. (2019). Comparative study of the binding mode between cytochrome P450 17A1 and prostate cancer drugs in the absence of haem iron. *Journal of Biomolecular Structure and Dynamics*, *37*(16), 4161–4170. https://doi.org/10.1080/07391102.2018.1540360

[35] Omoboyowa, D. A., Balogun, T. A., Saibu, O. A., Chukwudozie, O. S., Alausa, A., Olubode, S. O., …, & Musa, S. O. (2022). Structure-based discovery of selective $CYP_{17}A_1$ inhibitors for Castration-resistant prostate cancer treatment. *Biology Methods and Protocols*, *7*(1), bpab026. https://doi.org/10.1093/biomethods/bpab026

[36] Abdi, S. A. H., Ali, A., Sayed, S. F., Ahsan, M. J., Tahir, A., Ahmad, W., …, & Ali, A. (2021). Morusflavone, a new therapeutic candidate for prostate cancer by CYP17A1 inhibition: Exhibited by molecular docking and dynamics simulation. *Plants*, *10*(9), 1912. https://doi.org/10.3390/plants10091912

[37] Langevin, M., Minoux, H., Levesque, M., & Bianciotto, M. (2020). Scaffold-constrained molecular generation. *Journal*

of Chemical Information and Modeling, *60*(12), 5637–5646. https://doi.org/10.1021/acs.jcim.0c01015

[38] Hu, C., Li, S., Yang, C., Chen, J., Xiong, Y., Fan, G., . . . , & Hong, L. (2023). ScaffoldGVAE: Scaffold generation and hopping of drug molecules via a variational autoencoder based on multi-view graph neural networks. *Journal of Cheminformatics*, *15*(1), 91. https://doi.org/10.1186/s13321-023-00766-0

[39] Martin, Y. C. (2012). Hansch analysis 50 years on. *WIREs Computational Molecular Science*, *2*(3), 435–442. https://doi.org/10.1002/wcms.1096

[40] Tute, M. S. (1971). Principles and practice of Hansch analysis: A guide to structure-activity correlation for the medicinal chemist. *Advances in Drug Research*, *6*, 1–77.

[41] Hall, L. H., & Kier, L. B. (1978). Molecular connectivity and substructure analysis. *Journal of Pharmaceutical Sciences*, *67*(12), 1743–1747. https://doi.org/10.1002/jps.2600671229

[42] Gupta, A., Kumar, V., & Aparoy, P. (2018). Role of topological, electronic, geometrical, constitutional and quantum chemical based descriptors in QSAR: mPGES-1 as a case study. *Current Topics in Medicinal Chemistry*, *18*(13), 1075–1090. https://doi.org/10.2174/1568026618666180719164149

[43] Agarwal, D. S., Sakhuja, R., Beteck, R. M., & Legoabe, L. J. (2023). Steroid-triazole conjugates: A brief overview of synthesis and their application as anticancer agents. *Steroids*, *197*, 109258. https://doi.org/10.1016/j.steroids.2023.109258

[44] Alghamdi, S. S., Suliman, R. S., Almutairi, K., Kahtani, K., & Aljatli, D. (2021). Imidazole as a promising medicinal scaffold: Current status and future direction. *Drug Design, Development and Therapy*, *15*, 3289–3312. https://doi.org/10.2147/DDDT.S307113

[45] Owen, C. P., Dhanani, S., Patel, C. H., Shahid, I., & Ahmed, S. (2006). Synthesis and biochemical evaluation of a range of potent benzyl imidazole-based compounds as potential inhibitors of the enzyme complex 17α-hydroxylase/17, 20-lyase ($P450_{17\alpha}$). *Bioorganic & Medicinal Chemistry Letters*, *16*(15), 4011–4015. https://doi.org/10.1016/j.bmcl.2006.05.070

[46] Owen, C. P., Shahid, I., Olusanjo, M. S., Patel, C. H., Dhanani, S., & Ahmed, S. (2008). Synthesis, biochemical evaluation and rationalisation of the inhibitory activity of a range of phenyl alkyl imidazole-based compounds as potent inhibitors of the enzyme complex 17α-hydroxylase/17, 20-lyase ($P450_{17\alpha}$). *The Journal of Steroid Biochemistry and Molecular Biology*, *111*(1–2), 117–127. https://doi.org/10.1016/j.jsbmb.2008.05.007

[47] Boujonnier, F., Lemaitre, F., & Scailteux, L. M. (2024). Pharmacokinetic interactions between abiraterone, apalutamide, darolutamide or enzalutamide and antithrombotic drugs: Prediction of clinical events and review of pharmacological information. *Cardiovascular Drugs and Therapy*, *38*(4), 757–767. https://doi.org/10.1007/s10557-023-07453-0

[48] Lebouvier, N., Pagniez, F., Na, Y. M., Shi, D., Pinson, P., Marchivie, M., . . . , & le Borgne, M. (2020). Synthesis, optimization, antifungal activity, selectivity, and CYP51 binding of new 2-aryl-3-azolyl-1-indolyl-propan-2-ols. *Pharmaceuticals*, *13*(8), 186. https://doi.org/10.3390/ph13080186

[49] Ratre, P., Kulkarni, S., Das, S., Liang, C., Mishra, P. K., & Thareja, S. (2023). Medicinal chemistry aspects and synthetic strategies of coumarin as aromatase inhibitors: An overview. *Medical Oncology*, *40*(1), 41. https://doi.org/10.1007/s12032-022-01916-4

[50] Kędzierski, J., Jäger, M. C., Naeem, S., Odermatt, A., & Smieško, M. (2024). *In silico* and *in vitro* assessment of drugs potentially causing adverse effects by inhibiting CYP17A1. *Toxicology and Applied Pharmacology*, *486*, 116945. https://doi.org/10.1016/j.taap.2024.116945

[51] Avgeris, I., Pliatsika, D., Nikolaropoulos, S. S., & Fousteris, M. A. (2022). Targeting androgen receptor for prostate cancer therapy: From small molecules to PROTACs. *Bioorganic Chemistry*, *128*, 106089. https://doi.org/10.1016/j.bioorg.2022.106089

[52] Ahmed, S., Shahid, I., Dhanani, S., & Owen, C. P. (2009). Synthesis and biochemical evaluation of a range of sulfonated derivatives of 4-hydroxybenzyl imidazole as highly potent inhibitors of rat testicular 17α-hydroxylase/17, 20-lyase ($P\text{-}450_{17\alpha}$). *Bioorganic & Medicinal Chemistry Letters*, *19*(16), 4698–4701. https://doi.org/10.1016/j.bmcl.2009.06.070

[53] Patel, C. H., Dhanani, S., Owen, C. P., & Ahmed, S. (2006). Synthesis, biochemical evaluation and rationalisation of the inhibitory activity of a range of 4-substituted phenyl alkyl imidazole-based inhibitors of the enzyme complex 17α-hydroxylase/17, 20-lyase ($P450_{17\alpha}$). *Bioorganic & Medicinal Chemistry Letters*, *16*(18), 4752–4756. https://doi.org/10.1016/j.bmcl.2006.06.092

[54] Hansch, C., & Fujita, T. (1964). *p*-σ-π analysis. A method for the correlation of biological activity and chemical structure. *Journal of the American Chemical Society*, *86*(8), 1616–1626. https://doi.org/10.1021/ja01062a035

[55] Dassault Systèmes. (2020). *BIOVIA discovery studio: Comprehensive modeling and simulation for life sciences research*. Retrieved from: https://www.3ds.com/products/biovia/discovery-studio

[56] Zhao, L., Fu, L., Li, G., Yu, Y., Wang, J., Liang, H., . . . , & Wang, Y. (2023). Three-dimensional quantitative structural-activity relationship and molecular dynamics study of multivariate substituted 4-oxyquinazoline HDAC6 inhibitors. *Molecular Diversity*, *27*(3), 1123–1140. https://doi.org/10.1007/s11030-022-10474-w

[57] Achary, P. G. R. (2020). Applications of quantitative structure-activity relationships (QSAR) based virtual screening in drug design: A review. *Mini Reviews in Medicinal Chemistry*, *20*(14), 1375–1388. https://doi.org/10.2174/1389557520666200429102334

[58] Tomy, P. C., & Mohan, C. G. (2023). Chemical space navigation by machine learning models for discovering selective MAO-B enzyme inhibitors for Parkinson's disease. *Artificial Intelligence Chemistry*, *1*(2), 100012. https://doi.org/10.1016/j.aichem.2023.100012

[59] Bhowmik, R., Kant, R., Manaithiya, A., Saluja, D., Vyas, B., Nath, R., . . . , & Aspatwar, A. (2024). Navigating bioactivity space in anti-tubercular drug discovery through the deployment of advanced machine learning models and cheminformatics tools: A molecular modeling based retrospective study. *Frontiers in Pharmacology*, *14*, 1340724. https://doi.org/10.3389/fphar.2023.1340724

[60] van de Waterbeemd, H. (1995). *Chemometric methods in molecular design*. Germany: Wiley. http://doi.org/10.1002/9783527615452

[61] Roy, K. (2007). On some aspects of validation of predictive quantitative structure–activity relationship models. *Expert Opinion on Drug Discovery*, *2*(12), 1567–1577. https://doi.org/10.1517/17460441.2.12.1567

[62] Gramatica, P. (2007). Principles of QSAR models validation: Internal and external. *QSAR & Combinatorial Science*, *26*(5), 694–701. https://doi.org/10.1002/qsar.200610151

[63] Gramatica, P. (2013). On the development and validation of QSAR models. In B. Reisfeld & A. N. Mayeno (Eds.),

Computational toxicology (Vol. 2, pp. 499–526). Humana Press. https://doi.org/10.1007/978-1-62703-059-5_21

[64] Snedecor, G. W., & Cochran, W. G. (1967). *Statistical methods*. USA: The Iowa State University Press.

[65] Consonni, V., Ballabio, D., & Todeschini, R. (2009). Comments on the definition of the Q^2 parameter for QSAR validation. *Journal of Chemical Information and Modeling*, *49*(7), 1669–1678. https://doi.org/10.1021/ci900115y

[66] Schüller, A., Hähnke, V., & Schneider, G. (2007). SmiLib v2.0: A Java-based tool for rapid combinatorial library enumeration. *QSAR & Combinatorial Science*, *26*(3), 407–410. https://doi.org/10.1002/qsar.200630101

[67] Pathak, C., Matore, B. W., Singh, J., Roy, P. P., & Kabra, U. D. (2024). Discovery of potential 1, 2, 4-triazole derivatives as aromatase inhibitors for breast cancer: Pharmacophore modelling, virtual screening, docking, ADMET and MD simulation. *Molecular Simulation*, *50*(15), 1206–1219. https://doi.org/10.1080/08927022.2024.2390950

[68] Shivanika, C., Kumar, S. D., Ragunathan, V., Tiwari, P., Sumitha, A., & Devi, P. B. (2022). Molecular docking, validation, dynamics simulations, and pharmacokinetic prediction of natural compounds against the SARS-CoV-2 main-protease. *Journal of Biomolecular Structure and Dynamics*, *40*(2), 585–611. https://doi.org/10.1080/07391102.2020.1815584

How to Cite: Matore, B. W., Murmu, A., Singh, J., & Roy, P. P. (2025). Combinatorial Design of Imidazole/Triazole Linked Aryl-Substituted Derivatives as CYP17 Inhibitors Exploring Hansch and Molecular Docking Approach. *Medinformatics*, *2*(3), 205–218. https://doi.org/10.47852/bonviewMEDIN52024158